

Electrochemical Cleavage of N=N Bonds at a Mo₂(μ-SMe)₃ Site Relevant to the Biological Reduction of Dinitrogen at a Bimetallic Sulfur Centre

Nathalie Le Grand,^[a, b] Kenneth W. Muir,^[c] François Y. Pétilion,^[a] Christopher J. Pickett,^[b] Philippe Schollhammer,^[a] and Jean Talarmin^{*[a]}

Abstract: The reduction of diazene complexes [Mo₂Cp₂(μ-SMe)₃(μ-η²-H-N=N-R)]⁺ (R = Ph (**3a**); Me (**3b**)) and of the hydrazido(2-) derivative [Mo₂Cp₂(μ-SMe)₃{μ-η¹-N=N(Me)H}]⁺ (**1b**) has been studied by cyclic voltammetry, controlled-potential electrolysis, and coulometry in THF. The electrochemical reduction of **3a** in the presence of acid leads to cleavage of the N=N bond and produces aniline and either the amido complex [Mo₂Cp₂(μ-SMe)₃(μ-NH₂)] **4** or the ammine complex [Mo₂Cp₂(μ-SMe)₃(NH₃)(X)] **5**, depend-

ing on the initial concentration of acid (HX = HTsO or CF₃CO₂H). The N=N bond of the methylhydrazide analogue **3b** is not cleaved under the same conditions. The ability of **3a** but not **3b** to undergo reductive cleavage of the N=N bond is attributed to electronic control of the strength of the Mo-N(R) bond by

Keywords: dinuclear complexes • electrochemistry • molybdenum • N ligands • N=N bond cleavage • nitrogen fixation • S ligands

the R group. The electrochemical reduction of the methylhydrazido(2-) compound **1b** in the presence of HX also results in cleavage of the N=N bond, with formation of methylamine, **4** (or **5**) and the methylidiazenido complex [Mo₂Cp₂(μ-SMe)₃(μ-η¹-N=N-Me)]. Formation of the last of these complexes indicates that two mechanisms (N=N bond cleavage and possibly H₂ production) are operative. A pathway for the reduction of N₂ at a dinuclear site of FeMoco is proposed on the basis of these results.

Introduction

The determination of the structure^[1, 2] of the iron-molybdenum cofactor (FeMoco) of Mo nitrogenase has so far led neither to a clearer picture of how dinitrogen is activated on this cluster nor to improvements in the design of synthetic catalysts for N₂ reduction. Indeed, it is still a matter of debate which site on the cofactor binds and reduces molecular N₂. It may be mononuclear (and in this case the metal could be either Mo or Fe) or polynuclear. The octahedral geometry of the unique Mo centre has led some to question the role of molybdenum in N₂-binding and reduction.^[1a, 3, 4, 5c] However, in the crystal structure the molecule is in a redox state that is inactive toward N₂ reduction. Addition of the three electrons

required to activate the enzyme may be accompanied by substantial changes in the Mo coordination sphere. Recently, there has been strong support for the idea that the molybdenum centre of FeMoco is involved in N₂ binding and reduction.^[6, 7] The contrary view that the central array of coordinatively unsaturated Fe atoms might be the active site is supported by theoretical calculations, which modelled the coordination of dinitrogen to the trigonal prism of iron atoms.^[8-11] Although it is known from studies of functional models that two metal centres are not *essential* for the reduction of N₂ to ammonia,^[7, 12-16] these calculations also indicate that coordination of the substrate to several metal centres would *facilitate* cleavage of the N-N triple bond. Discussions about the participation of a second metal centre in chemical nitrogen fixation almost invariably refer^[5-a, b, 7, 12-16, 17c] to M(μ-L)M' complexes in which the two metal centres (which may be the same or different) are bridged only by the substrate L (L = N₂, N₂H₂, N₂H₄). Transformations (i.e. protonation, reduction) of the bridging substrate result in disruption of the dinuclear assembly at some stage of the reduction process, so that the utility of the second metal can be questioned in these models. One of these complexes did, however, lead to cleavage of the dinitrogen triple bond.^[17a, b]

Our approach involves a dinuclear site that is conceptually quite different. The possibility that Mo(μ-S)Fe or Fe(μ-S)Fe arrangements occur at the binding site on the cofactor^[5d, 21-23]

[a] Dr. J. Talarmin, Dr. N. Le Grand, Prof. F. Y. Pétilion, Dr. P. Schollhammer
UMR 6521 Chimie, Electrochimie Moléculaires et Chimie Analytique
Université de Bretagne Occidentale
6 Av. V Le Gorgeu B.P. 809, 29285 Brest Cedex (France)
E-mail: jean.talarmin@univ-brest.fr

[b] Dr. N. Le Grand, Prof. C. J. Pickett
Department of Biological Chemistry, John Innes Centre
Norwich Research Park, Colney, Norwich NR4 7UH (UK)

[c] Dr. K. W. Muir
Department of Chemistry, University of Glasgow
Glasgow G12 8QQ (UK)

has led us to investigate complexes with a robust $\{M_2(\mu-SR)_n\}$ unit ($M = V,^{[18b]} Mo,^{[18a]} W,^{[18a]} Fe,^{[18g]}$ $n = 2$ or 3). $\{Fe(\mu-SR)_2\}^{[18g, 19]}$ or $\{Ru(\mu-SR)_n\}^{[20]}$ cores can be seen as models for the metal sites of FeMoco, even though they do not bind dinitrogen. Besides our efforts to construct such a $\{M_2(\mu-SR)_n\}$ site capable of binding N_2 ,^[18] we are also interested in the transformation at dinuclear sites of nitrogenous ligands, which may be intermediates in the reduction of dinitrogen to ammonia. Because we wanted to explore the reactivity and the specificity of dinuclear sites in the transformation of diazo ligands, we attached as much importance to this characteristic as to the nature of the metal centres in the complexes; for this reason, we used $\{M(\mu-SR)_nM\}$ compounds ($M = Mo$ or W).^[18] One of the obvious roles of the bridging thiolate ligands in these species is to maintain the close proximity of the metal centres throughout the reaction sequence, thus preventing disruption of the dinuclear entity.^[24] The metal–metal separation, ranging from about 2.6 to 3 Å,^[18a, 26, 27] precludes linear $M(\mu-L)M'$ arrangements in these models. Instead, $\mu-\eta^2$ and nonlinear $\mu-\eta^1$ modes of substrate coordination are both possible,^[20, 27] as is terminal binding of the substrate to one of the metal atoms.^[18–20]

We have recently reported on the reactivity^[28] of the amide complex $[Mo_2Cp_2(\mu-SMe)_3(\mu-NH_2)]$, and have shown that the electrochemical reduction of the metal imide, $[Mo_2Cp_2(\mu-SMe)_3(\mu-NH)]^+$ in the presence of acid produces ammonia via the amide and ammine derivatives.^[29]

We now show that the $N=N$ bonds of $\mu-\eta^2-H-N=N-Ph$ and $\mu-\eta^1-N=N(Me)H$ ligands can be cleaved by electrochemical reduction of $[Mo_2Cp_2(\mu-SMe)_3(\mu-N_2HR)]^{+ [27, 30]}$ in the presence of acid. The reduction produces complexes in which an ammine or amide ligand is coordinated to the conserved $\{[Mo_2Cp_2(\mu-SMe)_3]^+\}$ core. We believe that these results give

Abstract in French: Les processus de réduction de complexes diazène $[Mo_2Cp_2(\mu-SMe)_3(\mu-\eta^2-H-N=N-R)]^+$ ($R = Ph$ (**3a**); Me (**3b**)) et hydrazido(2-) $[Mo_2Cp_2(\mu-SMe)_3(\mu-\eta^1-N=N(Me)H)]^+$ (**1b**) ont été étudiés dans le thf par voltammétrie cyclique, électrolyse à potentiel contrôlé et coulométrie. Alors que la réduction de **3a** en milieu acide conduit à la coupure de la liaison $N=N$ et à la formation d'aniline et des dérivés amidure $[Mo_2Cp_2(\mu-SMe)_3(\mu-NH_2)]$ **4** ou ammine $[Mo_2Cp_2(\mu-SMe)_3(NH_3)(X)]$ **5** selon la quantité initiale d'acide ($HX = H_2SO_4$ or CF_3CO_2H), la liaison $N=N$ de **3b** n'est pas coupée par réduction de ce complexe en présence de protons. Cette différence est attribuée à l'effet du substituant R ($R = Ph$ ou Me) sur la solidité de la liaison $Mo-N(R)$. La réduction du complexe méthylhydrazido(2-) **1b** en présence de protons conduit à la coupure de la liaison $N=N$ et à la formation du composé **4** (ou **5**) et du complexe diazénido $[Mo_2Cp_2(\mu-SMe)_3(\mu-\eta^1-N=N-Me)]$ précurseur de **1b**. La formation du dérivé diazénido indique la coexistence de deux mécanismes (coupure $N=N$ et vraisemblablement production de H_2) dans ce cas. Les résultats suggèrent une possible intervention de deux centres métalliques du FeMoco dans le processus de réduction de l'azote moléculaire par la nitrogénase.

new insight into the reduction of dinitrogen at a bimetallic sulfur-bridged site of FeMoco. Some of this work has already appeared in a preliminary form.^[31]

Results

Electrochemical reduction of $[Mo_2Cp_2(\mu-SMe)_3(\mu-\eta^2-HNNPh)]^+$, **3a:** We have previously reported the synthesis of three different isomers of $[Mo_2Cp_2(\mu-SMe)_3(\mu-N_2HPh)]^+$, in which the diazo ligand is bound to the metal core in the $\mu-\eta^1$ (**1a**) and in the $\mu-\eta^2$ mode (**2a, 3a**).^[27, 30] The conversion of the phenylhydrazido(2-) complex **1a** to the $\mu-\eta^2$ isomer **3a**, occurs via the third isomer **2a**, which differs from **3a** by the relative disposition of the equatorial SMe groups (**2a**, *anti*: “up–down”; **3a**, *syn*: “up–up”).^[27] Since **1a** would be converted to a mixture of the different isomers by the thermal process on the electrolysis time scale, we decided to focus our electrochemical study on the final isomer, **3a**. However, the redox potentials of **1a** and **2a** are also listed in Table 1.

Table 1. Redox potentials of $[Mo_2Cp_2(\mu-SMe)_3(\mu-N_2HR)]^+$ complexes (CV measurements in THF/[NBu₄][PF₆], V/Fc).

Compound	E_p^{red}	$E_{1/2}^{ox1}$	$E_{1/2}^{ox2}$
$[Mo_2Cp_2(\mu-SMe)_3(\mu-\eta^1-NNHPh)]^+$ (1a)	–1.56	0.2 (irr) ^[a]	
$[Mo_2Cp_2(\mu-SMe)_3(\mu-\eta^2-HNNPh)]^+$ (2a)	–1.65	–0.11	0.89 (irr)
$[Mo_2Cp_2(\mu-SMe)_3(\mu-\eta^2-HNNPh)]^+$ (3a)	–1.63 ($E_{1/2}$)	0	0.89 (irr)
$[Mo_2Cp_2(\mu-SMe)_3(\mu-\eta^1-NNHMe)]^+$ (1b)	–1.90	0.07 (irr)	
$[Mo_2Cp_2(\mu-SMe)_3(\mu-\eta^2-HNNMe)]^+$ (2b)	–1.88	–0.15	0.78 (irr)
$[Mo_2Cp_2(\mu-SMe)_3(\mu-\eta^2-HNNMe)]^+$ (3b)	–1.94	–0.05	0.74 (irr)

[a] irr = irreversible.

The cyclic voltammetry (CV^[32]) of **3a** shows three reduction processes in THF/[NBu₄][PF₆] at $E_{1/2}^{red1} = -1.63$, $E_p^{red2} = -2.9$, and $E_p^{red3} \approx -3.2$ V. The latter two reductions were not investigated. The first reduction (Figure 1) is a diffusion-controlled one-electron step (by comparison of the reduction peak current, i_p^{red1} , to the peak current of the reversible^[33] oxidation, i_p^{ox} : the ratio $i_p^{red1}/i_p^{ox} \approx 1.1$; Figure 1); the electron

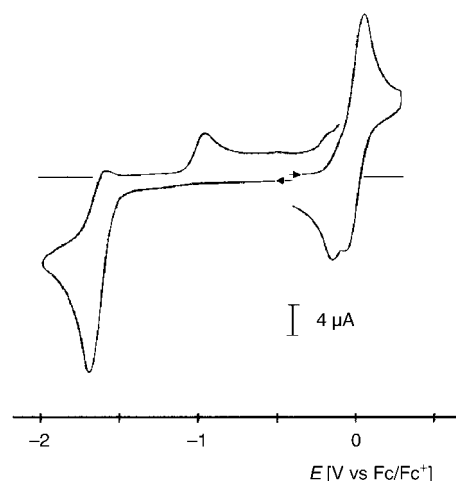
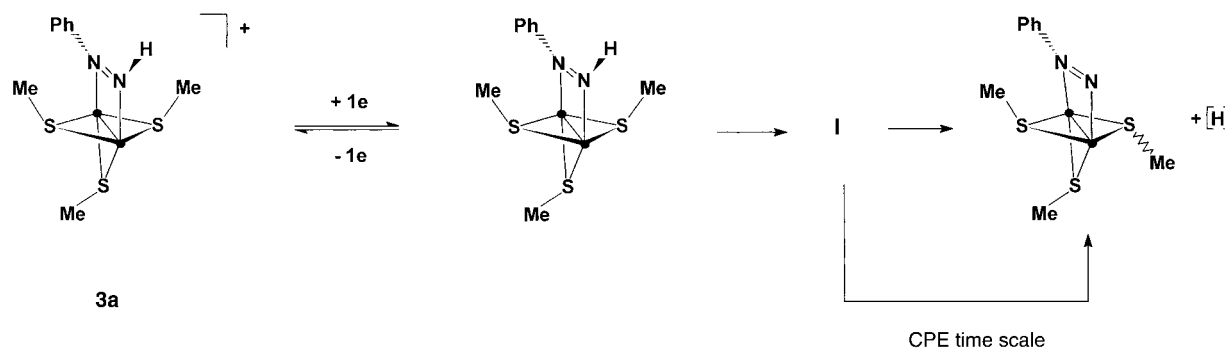


Figure 1. Cyclic voltammetry of $[Mo_2Cp_2(\mu-SMe)_3(\mu-\eta^2-HN=NPh)]^+$ (**3a**; about 0.8 mm) in THF/[NBu₄][PF₆] (vitreous carbon electrode, $v = 0.2$ V s⁻¹).

transfer is coupled to chemical reaction(s) affording a product that is irreversibly oxidizable at -0.95 V (EC process^[32, 35]). Partial reversibility of the first reduction of **3a** is obtained on increasing the scan rate or on decreasing the temperature ($\nu = 0.2$ V s⁻¹, $T = -40$ °C, THF electrolyte, $\Delta E_p^{\text{red}} = 80$ mV, $(i_p^{\text{a}}/i_p^{\text{c}})^{\text{red}} = 0.45$). Under these conditions, the ratio of the peak current of the oxidation at -0.95 V to i_p^{red1} is slightly decreased. The rate constant of the chemical reaction following the electron transfer was determined in THF at 20 °C using the method of Nicholson and Shain:^[36] $k_{\text{obs}} = 1.5 \pm 0.1$ s⁻¹. The peak current ratio of the first two reductions, $i_p^{\text{red2}}/i_p^{\text{red1}}$, decreases on lowering the temperature ($(i_p^{\text{red2}}/i_p^{\text{red1}}) = 0.9$ at 20 °C and about 0.5 at -40 °C, THF electrolyte). This indicates that the peak around -2.9 V is due to a product generated by the first reduction.

Controlled-potential reduction at -1.8 V (THF/[NBu₄][PF₆], Pt cathode) quantitatively produced the neutral μ - η^2 -phenyldiazenido complex^[37] after 0.9 ± 0.1 F mol⁻¹ of **3a** had been consumed. The species responsible for the oxidation at -0.95 V was not present after electrolysis so we assigned it as an intermediate (**I**) of the reduction process. Plots of the cell current versus the charge passed show that the charge extrapolated from the early stages of the electrolysis is close to 2 F mol⁻¹ of **3a**, but after about 0.5 F mol⁻¹ **3a** has been consumed, the curve deviates markedly from linearity and the electrolysis ends after consumption of approximately 1 F mol⁻¹ of **3a**. Therefore, although the overall stoichiometry and the product of the electrochemical reduction are consistent with the one-electron process in Scheme 1, it is clear that [Mo₂Cp₂(μ -SMe)₃(μ - η^2 -NNPh)] does not arise simply from the loss of an hydrogen atom from either the phenyldiazene radical or intermediate **I**.^[38] The latter must be involved in reactions that are too slow for detection by CV. The nature of the reaction or reactions converting **I** to the final product on the electrolysis time scale is unknown.

Reduction of [Mo₂Cp₂(μ -SMe)₃(μ - η^2 -HNNPh)]⁺ (3a**) in the presence of acid:** The stepwise addition of acid (*p*-toluenesulfonic acid, HTsO or trifluoroacetic acid, CF₃CO₂H) to a THF/[NBu₄][PF₆] solution of **3a** was monitored by cyclic voltammetry. This showed that the peak current (i_p^{ox}) of the reversible oxidation of the complex at $E_{1/2}^{\text{ox}} = 0$ V was not affected by the addition of acid, which demonstrates that **3a** is not protonated. Furthermore, the first reduction is irreversible in the presence of protons at scan rates at which some



Scheme 1. ● = MoCp.

reversibility was observed in the absence of acid; i_p^{red1} increases substantially until about one equivalent of acid has been added (1 equiv H⁺, $(i_p^{\text{red1}}/i_p^{\text{ox}}) = 2$ for $\nu = 0.02$ V s⁻¹; 1.7 for $\nu = 0.2$ V s⁻¹), while a smaller increase is noted for further additions. This is consistent with the occurrence of an ECE mechanism^[32, 35] in the presence of acid, where the chemical step is the protonation of the primary reduction product. Owing to the short lifetime of [Mo₂Cp₂(μ -SMe)₃(μ - η^2 -HNNPh)][•] in the absence of acid ($t_{1/2} \approx 0.5$ s), its reaction product (intermediate **I**; Scheme 1) could also be protonated. The fact that addition of acid resulted in the suppression of the redox process of **I** at -0.95 V shows that either **I** is protonated, or that its formation is prevented by protonation of its precursor.

The plot of the current function $i_p^{\text{red1}}/\nu^{1/2}$ versus scan rate (Figure 2) reveals two important points. First, the ratio of the current function measured at a scan rate $\nu = 1$ V s⁻¹ in the presence of acid to that measured in the absence of acid is 1.5 (1 equiv H⁺) or 1.6 (2 equiv H⁺). Secondly, this ratio increases

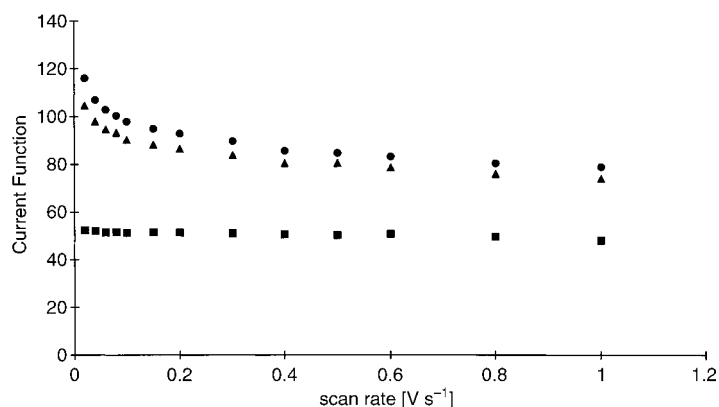


Figure 2. Plots of the current function ($i_p^{\text{red1}}/\nu^{1/2}$) for the first reduction against scan rate (ν) in the absence of acid (■), and in the presence of one equivalent (▲), and two equivalents HTsO (●) (THF/[NBu₄][PF₆]; vitreous carbon electrode).

to 2 (1 equiv H⁺) or 2.2 (2 equiv H⁺) at slow scan rates (0.02 V s⁻¹). This indicates that 1) the initial electron transfer is followed by a fast protonation step, which produces a species reducible at a potential less negative than, or equal to, that of **3a** (ECE mechanism); this sequence causes the loss of reversibility of the first reduction and the increase of the reduction current observed at scan rates $\nu \geq$ of about

0.4 V s⁻¹. 2) The species that results from the ECE process undergoes slower chemical reactions followed by further electron transfer steps detected by CV at slower scan rates ($\nu < 0.2$ V s⁻¹, Figure 2). The rate constant of the first chemical step was estimated as $k = 25 \pm 5$ s⁻¹ from the values of the current function (0.6 V s⁻¹ $\leq \nu \leq 1$ V s⁻¹) in the absence and in the presence of protons, using the method of Nicholson and Shain.^[39]

New peaks arising from the product of the 1H⁺/2e sequence (first ECE process) are observed around -2.3 V and -2.5 V (irreversible reduction) and -0.32 V (irreversible oxidation, Figure 3a). Variable scan rate- and “ramp-clamp” CV demonstrate that the species oxidizable at -0.32 V is the precursor of a complex with $E_{1/2}^{\text{ox}} = -0.6$ V (HTsO, Figure 3b), or -0.58 V (CF₃CO₂H). These potentials are coincident with those of the first oxidation of [Mo₂Cp₂(μ -SMe)₃(NH₃)(X)] (**5**; **5a**, X = TsO or **5b**, X = CF₃CO₂).^[28]

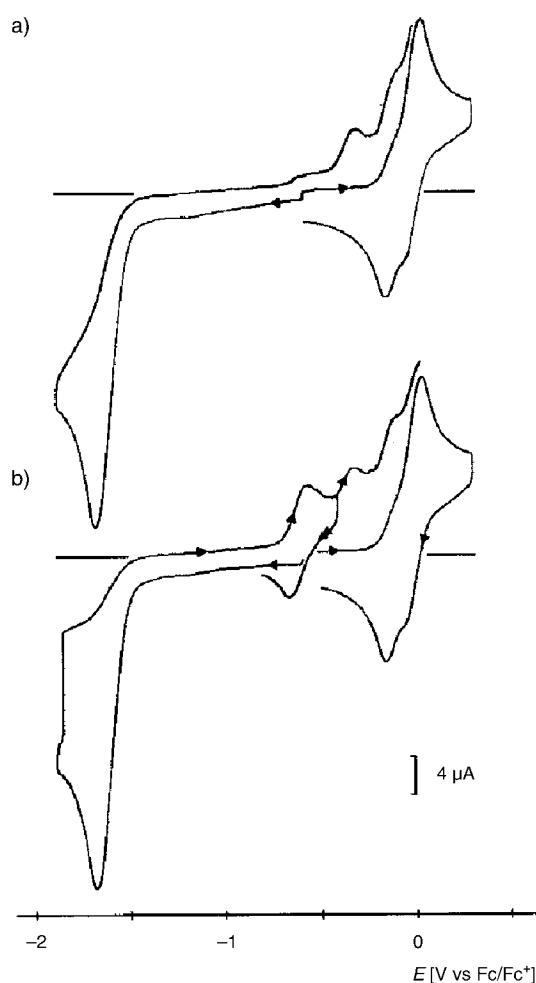


Figure 3. Cyclic voltammetry (a), and “ramp-clamp” CV (b) of [Mo₂Cp₂(μ -SMe)₃(μ - η^2 -HN=NPh)]⁺ (**3a**; about 1.2 mM) in THF/[NBu₄][PF₆] in the presence of three equivalents HTsO. In b), the potential was held at -1.8 V for 20 s before scan reversal (vitreous carbon electrode, $\nu = 0.2$ V s⁻¹).

Controlled-potential electrolyses at a Pt or graphite cathodes were performed at -1.8 V in the presence of various amounts of acid (HTsO or CF₃CO₂H). Electrolyses carried

out in the presence of one equivalent HTsO (1.8 F mol⁻¹ of **3a**) and two equivalents HTsO (2.8 F mol⁻¹ of **3a**) afforded mixtures of [Mo₂Cp₂(μ -SMe)₃(μ - η^2 -NNPh)] and [Mo₂Cp₂(μ -SMe)₃(μ -NH₂)] (**4**), characterised by their redox potentials and by comparison of the ¹H NMR spectra of the solid isolated from the catholyte with those of authentic samples of these compounds. The presence of **4** demonstrates unambiguously that the N=N bond of the diazo ligand has been reductively cleaved. An unidentified minor species with a quasireversible oxidation around -0.8 V, already observed after reduction of [Mo₂Cp₂(μ -SMe)₃(μ -NH)]⁺,^[29] was also present. Cyclic voltammetry of the catholyte after controlled-potential reduction in the presence of 3–3.5 equivalents HTsO ($n = 3.7 \pm 0.2$ F mol⁻¹ **3a**) showed that the amide complex **4** was the major product (about 75%^[37]) formed along with [Mo₂Cp₂(μ -SMe)₃(μ - η^2 -NNPh)]; the minor species with $E_{1/2}^{\text{ox}} \approx -0.8$ V was again observed (Figure 4). Controlled-potential reduction of **3a** in the presence of six equivalents HTsO afforded [Mo₂Cp₂(μ -SMe)₃(NH₃)(TsO)] (**5a**) in approximately 80% yield,^[37] after consumption of 6.4 F mol⁻¹ of **3a** (Scheme 2). Compound **5a** was characterised by its redox potentials and by its reaction with a base, which produces **4**.^[28]

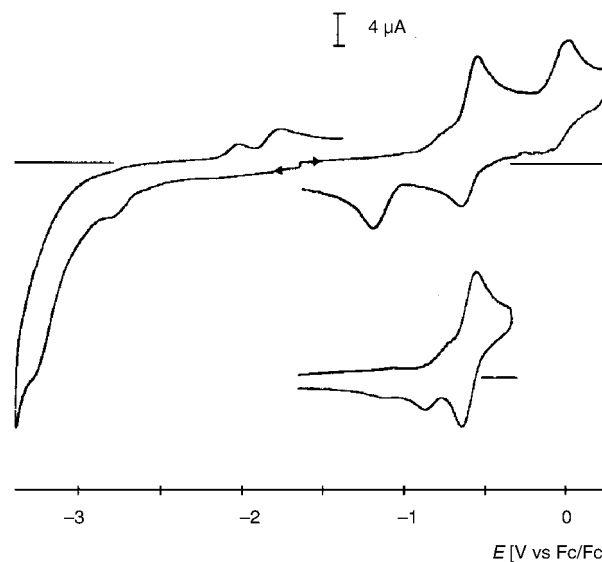
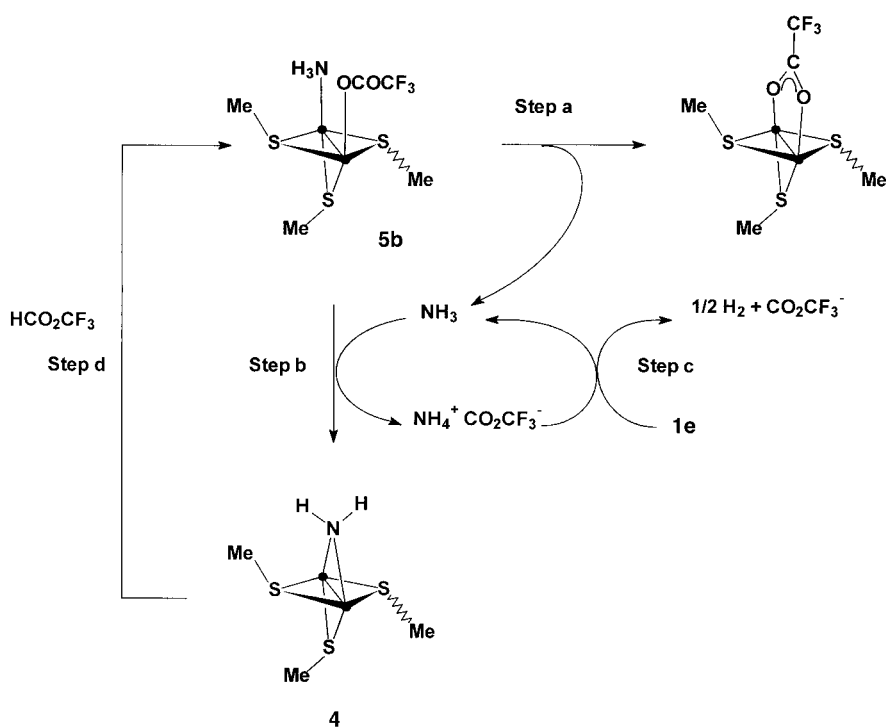


Figure 4. Cyclic voltammetry of the catholyte after controlled-potential reduction (Pt cathode; $E = -1.8$ V; 3.7 F mol⁻¹ **3a**) of [Mo₂Cp₂(μ -SMe)₃(μ - η^2 -HN=NPh)]⁺ (**3a**; about 0.6 mM) in the presence of three equivalents HTsO. The small reduction peak around -2.9 V is assigned to [Mo₂Cp₂(μ -SMe)₃(μ - η^2 -N=NPh)] (THF/[NBu₄][PF₆] vitreous carbon electrode, $\nu = 0.2$ V s⁻¹).

When CF₃CO₂H was used instead of HTsO, results similar to those described above were obtained, except that the minor species with a quasireversible oxidation around -0.8 V was not present. Cyclic voltammetric monitoring of electrolyses performed in the presence of four–six equivalents CF₃CO₂H showed that [Mo₂Cp₂(μ -SMe)₃(NH₃)(CF₃CO₂)] (**5b**), characterised by its redox potential and by its reaction with a base,^[28] formed steadily from the beginning of the electrolysis. A reversible oxidation around -0.35 V indicated the presence of [Mo₂Cp₂(μ -SMe)₃(μ -OCOFC₃)]^[41] as a by-product of the electrolyses (Figure 5b). This species was also obtained along



Scheme 3. ● = MoCp.

During the electrolyses in the presence of acid, protonation of **4** (Scheme 3, step d) regenerates **5b**, as long as protons are available in solution. The reactions in Scheme 3 (steps b–d) constitute a possible path for the reduction of protons, which is indicated by coulometry during the electrolysis of **3a**. When the excess protons have been consumed, **4** is produced (Scheme 3, step b); the formation of $[\text{Mo}_2\text{Cp}_2(\mu\text{-SMe})_3(\mu\text{-}\eta^2\text{-NNPh})]$ at the end of electrolyses of **3a** performed in the presence of four (or fewer) equivalents of acid is possibly due to the deprotonation of the diazene complex **3a** by ammonia.

From these experiments, it appears that the release of ammonia from **5b** may explain why the reduction of $[\text{Mo}_2\text{Cp}_2(\mu\text{-SMe})_3(\mu\text{-}\eta^2\text{-HNNPh})]^+$ exceeds the limiting stoichiometry in Scheme 2. The course of the controlled-potential reduction of **3a** in the presence of HX is similar for $\text{X} = \text{TsO}$ and CO_2CF_3 . In particular, the conversion of **5a** to the $\mu\text{-NH}_2$ derivative **4** at the end of electrolyses performed in the presence of HTsO suggests that ammonia is also released from $[\text{Mo}_2\text{Cp}_2(\mu\text{-SMe})_3(\text{NH}_3)(\text{TsO})]$, **5a**. Although the by-products of the reduction were not identified, $[\text{Mo}_2\text{Cp}_2(\mu\text{-SMe})_3(\text{L})(\text{TsO})]$ ($\text{L} = \text{H}_2\text{O}$ or thf) or $[\text{Mo}_2\text{Cp}_2(\mu\text{-SMe})_3(\mu\text{-TsO})]$ are reasonable possibilities.^[29]

Proposed mechanism for the cleavage of the N=N bond by reduction of 3a in the presence of protons: The electrochemical cleavage of the N=N bond in **3a** produces $[\text{Mo}_2\text{Cp}_2(\mu\text{-SMe})_3(\mu\text{-NH}_2)]$ and aniline in an overall (theoretical) $3\text{H}^+/4\text{e}^-$ process (Scheme 2); no intermediates can be isolated since they must be reducible at potentials less negative than that of the starting material, **3a**. However, the similarity of the products formed by reduction of **3a** and by reduction of the imide complex $[\text{Mo}_2\text{Cp}_2(\mu\text{-SMe})_3(\mu\text{-NH})]^{+29}$ suggests that the latter (or its reduced form) might be involved

as an intermediate in the reduction of **3a**. The variation of the current function with scan rate (Figure 2) demonstrates that successive ECE mechanisms are operative. These will be discussed separately.

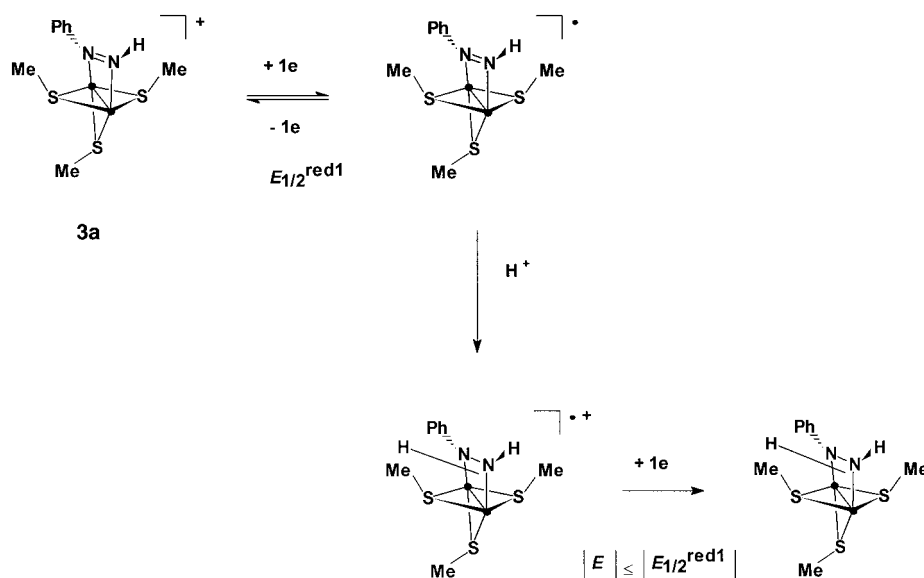
The first ECE mechanism: The initial step of the process leading to the cleavage of the N=N bond consists of the protonation of a species generated by reduction of **3a**. If the mechanism of the reduction were the same, irrespective of whether acid is present or absent, one would expect the electrolysis to result in the catalytic reduction of protons to dihydrogen, with $[\text{Mo}_2\text{Cp}_2(\mu\text{-SMe})_3(\mu\text{-}\eta^2\text{-NNPh})]$ as the only metal product. The formation of products arising from the N=N bond cleavage, namely $[\text{Mo}_2\text{Cp}_2(\mu\text{-SMe})_3(\mu\text{-NH}_2)]$ or $[\text{Mo}_2\text{Cp}_2(\mu\text{-SMe})_3(\text{NH}_3)(\text{X})]$ and PhNH_2 , demonstrates that a different mechanism operates when acid is present.

The change in the course of the reduction of **3a** caused by the presence of acid HX ($\text{X} = \text{TsO}$ or CF_3CO_2) must arise from the protonation of $[\text{Mo}_2\text{Cp}_2(\mu\text{-SMe})_3(\mu\text{-}\eta^2\text{-HNNPh})]^+$ (and possibly of intermediate **I**). This is shown by the loss of reversibility of the reduction of **3a** in the presence of acid at scan rates where some reversibility was observed in the absence of acid (Scheme 4).

Several protonation sites may be considered, the two nitrogen atoms and the lone pairs of the three bridging sulfur atoms. EHMO calculations were carried out on the diazene radical, assuming that the electron-transfer step causes no structural change^[42] with respect to the structurally characterised^[27] parent, **3a**. The calculated net charges of the atoms suggest that the N atoms are more susceptible to proton attack ($\text{N}(\text{H}): -0.63$; $\text{N}(\text{Ph}): -0.61$) than the S atoms ($S_{\text{equatorial}}: -0.10, -0.11$; $S_{\text{apical}}: -0.12$). Therefore, protonation at a N atom followed by one-electron reduction produces a phenylhydrazido(1–) complex **A**, **B**, or **C** (Scheme 5).

Interconversion of protons^[43] or of alkyl groups^[44] on the nitrogen atoms of mononuclear side-on bonded hydrazido(1–) complexes has been reported. In $[\text{W}(\text{Cp}^*)\text{Me}_4(\eta^2\text{-NHNH}_2)]$, two different fluxional processes take place.^[43] The lower energy one consists in a proton shift from one N atom to the other. The higher energy proton process interconverts H_B and H_C and is thought to occur through the $\eta^1\text{-NHNH}_2$ geometry (Scheme 6, $\text{R} = \text{H}$, $\text{M} = \{\text{W}(\text{Cp}^*)\text{Me}_4\}$, $\Delta G^\ddagger = 53 \text{ kJ mol}^{-1}$).^[43] A similar site-exchange mechanism was reported for $[\text{MoCp}(\text{NMeNMe}_2)\text{I}(\text{NO})]$ ($\text{R} = \text{Me}$, $\text{M} = \{\text{MoCpI}(\text{NO})\}$, $\Delta G^\ddagger = 59 \text{ kJ mol}^{-1}$, Scheme 6).^[44]

If similar fluxional processes take place for $[\text{Mo}_2\text{Cp}_2(\mu\text{-SMe})_3(\mu\text{-N}_2\text{H}_2\text{Ph})]$, species **A** and **B** would be related by

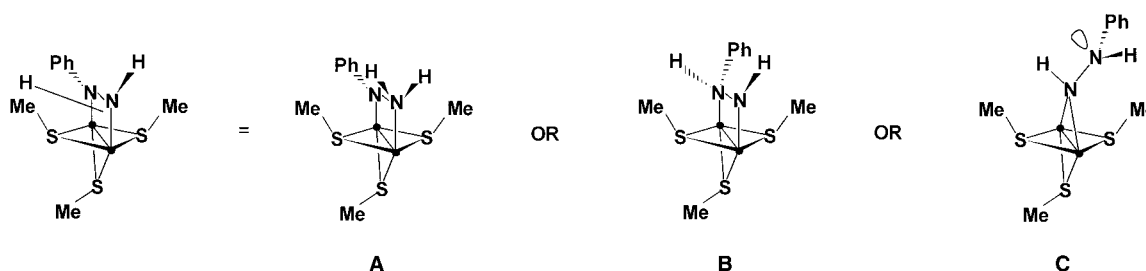


Scheme 4. ● = MoCp.

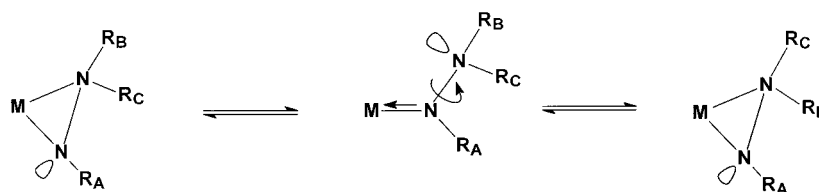
a proton 1,2-shift, while **C** would arise from a Mo–N–N–Mo ring opening analogous to the one depicted in Scheme 6. Formation of $[\text{TiCpCl}_2(\eta^2\text{-NPhNH}_2)]$ from $[\text{TiCpCl}_3]$ and $\text{SiMe}_3\text{NHNHPh}$ also indicated that a proton 1,2-shift occurred.^[45]

The second proton/electron-transfer mechanism: The reduction steps subsequent to the initial ECE process are detected by the increase of the current function at slow scan rates (Figure 2). The mechanism accounting for the “middle part” of the reduction of **3a** must therefore satisfy the condition that the initial ECE process is isolated from the following chemistry by a slow step. Protonation of nitrogenous ligands can be slow when the N lone pairs are engaged in bonding with metal atoms.^[46, 47]

The observation that the reducible species arising from the phenylhydrazido(1–) intermediate **A**, **B**, or **C** in Scheme 5 is formed by a chemical step, which is slower than the preceding one (i.e. protonation in Scheme 4), suggests that a rearrange-



Scheme 5. ● = MoCp.



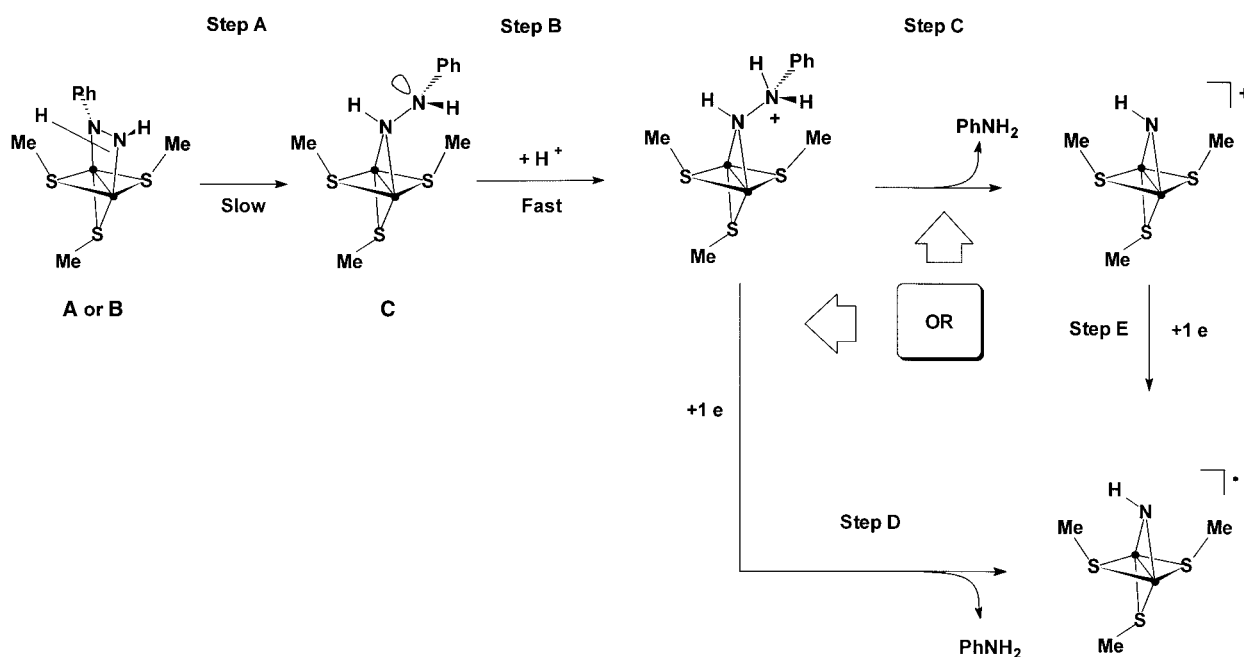
Scheme 6.

ment might be involved. Complex **C** is a possible intermediate of the N=N bond cleavage pathway since decoordination of the N(Ph) end of the diazo ligand is indicated by the nature of the electrolysis products. Indeed, we have never observed the formation of a product such as $[\text{Mo}_2\text{Cp}_2(\mu\text{-SMe})_3(\mu\text{-NHPH})]$, which would result from the cleavage of the N–N bond in a $\mu\text{-}\eta^2\text{-}$ coordinated ligand, or from the decoordination of the N(H) end of the ligand. Protonation of **C**, which has a lone pair of electrons available at N β , is expected to be fast. However, its formation from **A** or **B** (step A, Scheme 7), which requires a $\eta^2 \rightarrow \eta^1$ rearrangement, could

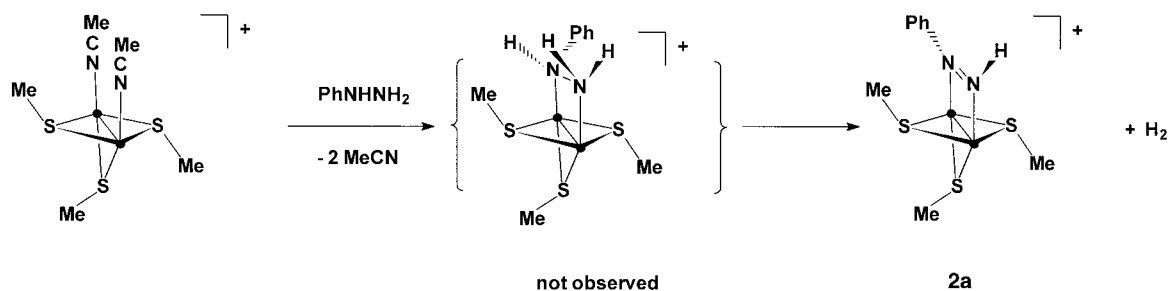
be the slow step isolating the initial ECE process from the following proton/electron transfers.

The first two steps in Scheme 7 are analogous to the protonation of the ligand in $[\text{Mo}(\text{S}_2\text{CNMe}_2)_2(\eta^2\text{-NHNMePh})(\text{N}_2\text{MePh})]^+$ and in $[\text{Ta}(\text{S}_2\text{CNEt}_2)_3(\eta^2\text{-NMeNMe}_2)]^+$, which involves the rate-determining opening of the MNN ring ($\eta^2 \rightarrow \eta^1$ rearrangement, see Scheme 6) before subsequent fast protic attack can take place at the remote N atom.^[46, 49]

The N–N bond might be cleaved as shown in Scheme 7, step C. However, several examples in the literature show that protonation of hydrazido(1–) ligands does not necessarily lead to N–N bond cleavage. The protonated ligand can be released as hydrazine^[45, 46, 49–52] (protonated or not) or kept in the metal coordination sphere as an η^2 hydrazine ligand.^[16b, 44] In the case of Schrock's complexes, protonation of $[\text{W}(\text{Cp}^*)\text{Me}_3(\eta^2\text{-NHNH}_2)]$ produces the η^2 -hydrazine derivative $[\text{W}(\text{Cp}^*)\text{Me}_3(\eta^2\text{-NH}_2\text{NH}_2)]^+$. A very elegant mechanism for the N–N bond cleavage in the one-electron reduced species has been proposed.^[16b] This involves the migration of



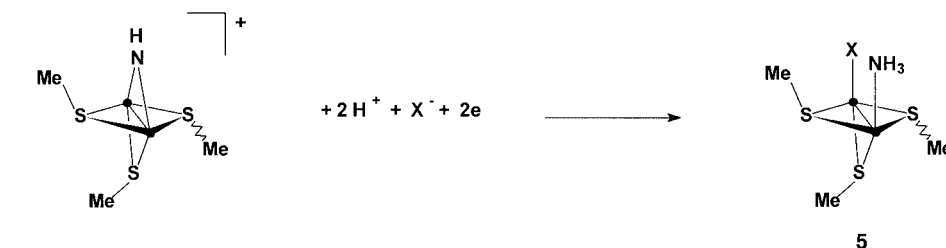
Scheme 7. ● = MoCp.



Scheme 8. ● = MoCp.

one of the NH_2 protons of the η^2 -hydrazine ligand to the metal, followed by a rearrangement of the resulting hydrido-hydrazido(1-) complex to an η^1 geometry. Eventually, migration of the M-H proton to the lone pair exposed on the terminal nitrogen by the $\eta^2 \rightarrow \eta^1$ structural change causes the N-N bond cleavage.^[16b] It is possible that in our dinuclear complexes, cleavage of the N-N bond also requires one-electron reduction of $[\text{Mo}_2\text{Cp}_2(\mu\text{-SMe})_3(\mu\text{-}\eta^1\text{-NHNH}_2\text{Ph})]^+$ (Scheme 7, step D).

If no $\eta^2 \rightarrow \eta^1$ rearrangement took place, protonation of the N(R) atom in **A** or **B** ($\text{R} = \text{Ph}$ or H , respectively) would produce a cation with an η^2 -bound phenylhydrazine ligand, $[\text{Mo}_2\text{Cp}_2(\mu\text{-SMe})_3(\mu\text{-}\eta^2\text{-NH}_2\text{NHPh})]^+$. This complex, which should also be the product formed first when $[\text{Mo}_2\text{Cp}_2(\mu\text{-SMe})_3(\text{MeCN})_2]^+$ is reacted with phenylhydrazine, was not observed in this reaction.^[30] Instead, the phenyldiazene complex **2a** (Scheme 8) was isolated along with variable (generally low) yields of an amidato complex resulting from hydration of

Scheme 9. ● = MoCp; $\text{X} = \text{TsO}$ or CF_3CO_2 .

one of the MeCN ligands of the reactant.^[53] The formation of **2a** therefore suggests that $[\text{Mo}_2\text{Cp}_2(\mu\text{-SMe})_3(\mu\text{-}\eta^2\text{-NH}_2\text{NHPh})]^+$ is not stable toward elimination of H_2 .

This might also be a pathway for H_2 production during the reduction of **3a** in the presence of acid. Dihydrogen loss as a consequence of the treatment of metal complexes with hydrazines has already been observed.^[48]

The final proton/electron-transfer steps: The successive proton- and electron-transfer steps discussed above generate the neutral or cationic μ -imido species (Scheme 7). The reduction of the latter to $[\text{Mo}_2\text{Cp}_2(\mu\text{-SMe})_3(\text{NH}_3)(\text{X})]$ (Scheme 9) has been described in detail elsewhere.^[29]

Reduction of $[\text{Mo}_2\text{Cp}_2(\mu\text{-SMe})_3\{\mu\text{-}\eta^1\text{-NNH(Me)}\}]^+$ (1b**) and $[\text{Mo}_2\text{Cp}_2(\mu\text{-SMe})_3(\mu\text{-}\eta^2\text{-HNNMe})]^+$ (**3b**) in the presence of acid:** The above results indicate that a rearrangement of the initially $\mu\text{-}\eta^2$ ligand to a $\mu\text{-}\eta^1$ geometry occurred during the reduction of **3a** in acidic medium. This suggests that reduction of the hydrazido(2-) (or isodiazeno) isomer in the presence of acid would lead more directly to N–N bond cleavage. Since the phenylhydrazido(2-) complex **1a** could not be used because of its conversion to the diazene isomers on the electrolysis time scale (see above), we investigated the methyl analogue (redox potentials in Table 1), whose isomerisation to the methyl diazene form is much slower.^[30] Controlled-potential reduction of $[\text{Mo}_2\text{Cp}_2(\mu\text{-SMe})_3\{\mu\text{-}\eta^1\text{-NNH(Me)}\}]^+$ **1b** at the potential of its first, irreversible reduction produces the diazenido derivative $[\text{Mo}_2\text{Cp}_2(\mu\text{-SMe})_3(\mu\text{-}\eta^1\text{-NNMe})]$ quantitatively, after consumption of about 1.2 F mol^{-1} of **1b**. This is similar to the result obtained for the reduction of **3a** in the absence of acid (Scheme 1). Dihydrogen is also a likely coproduct of the reduction of **1b**.^[38] Cyclic voltammetry of **1b** in THF/ $[\text{NBu}_4][\text{PF}_6]$ showed that addition of acid resulted in an increase of the reduction current,^[54] consistent with an ECE-type mechanism, while new redox processes due to products were detected on the return scan. Controlled-potential electrolyses carried out under these conditions (1 equiv $\leq \text{CF}_3\text{CO}_2\text{H} \leq 4$ equiv) led to a mixture of two compounds, the diazenido complex and $[\text{Mo}_2\text{Cp}_2(\mu\text{-SMe})_3(\mu\text{-NH}_2)]$, **4**, after consumption of 2.6 to 4 F mol^{-1} of **1b**, depending on the initial amount of acid. The products were identified by their redox potentials and by comparison of the ^1H NMR spectra of the solid isolated from the catholyte with those of authentic samples of these compounds. The presence of both products in the catholyte, even when the electrolyses were performed in the presence of an excess acid (4 equiv), suggests that two different mechanisms are operative. One of these produces $[\text{Mo}_2\text{Cp}_2(\mu\text{-SMe})_3(\mu\text{-}\eta^1\text{-NNMe})]$ and presumably H_2 , while the formation of **4** demonstrates that the N–N bond is cleaved on reduction in the presence of acid. Furthermore, the methylammonium cation (about 40 mol% with respect to **1b**) was detected by UV/Vis spectrometry of the catholyte (Scheme 10).

In contrast, controlled-potential reduction of $[\text{Mo}_2\text{Cp}_2(\mu\text{-SMe})_3(\mu\text{-}\eta^2\text{-HNNMe})]^+$ **2b** or **3b** in the presence of acid did not produce **4**, which demonstrates that the N–N bond was not cleaved. $[\text{Mo}_2\text{Cp}_2(\mu\text{-SMe})_3(\mu\text{-}\eta^2\text{-NNMe})]$ was recovered along with a species that could not be separated from the supporting electrolyte and was therefore not characterised. The failure of the electrolyses to cleave the N–N bond is also confirmed by CV of the catholyte, which shows that irrever-

sible oxidation of the unknown product regenerates the starting material (**2b** or **3b**).

Discussion and Conclusion

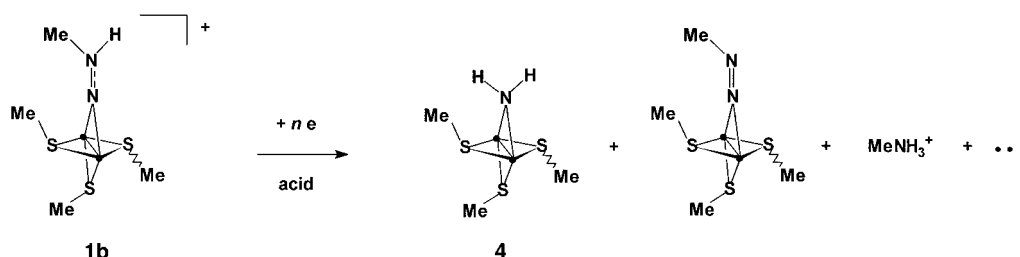
Reduction of nitrogenous ligands at the $\{\text{Mo}_2\text{Cp}_2(\mu\text{-SMe})_3\}^+$ site: The results presented above emphasise the effect both of the coordination mode of the N_2HR ligand at the $\{\text{Mo}_2\text{Cp}_2(\mu\text{-SMe})_3\}^+$ core and of the R substituent on the mechanism and products of the electrochemical reduction in the presence of protons.

First, the reduction of $[\text{Mo}_2\text{Cp}_2(\mu\text{-SMe})_3(\mu\text{-N}_2\text{HMe})]^+$ is clearly affected by the coordination mode of the diazo ligand. The N=N bond is reductively cleaved only when the ligand adopts a $\mu\text{-}\eta^1$ coordination (hydrazido(2-) or isodiazeno: **1b**), even though concurrent mechanisms producing the $\mu\text{-}\eta^1$ -diazenido derivative also take place. In the case of the $\mu\text{-}\eta^2$ coordination mode (diazene: **2b** or **3b**), no product resulting from the N=N bond cleavage could be detected.

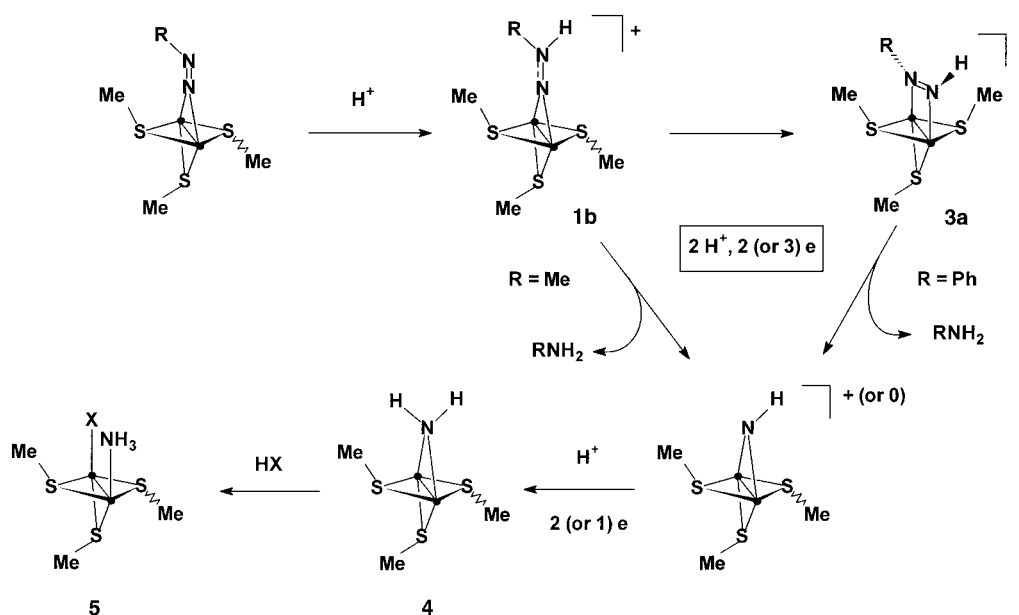
In contrast to the $\mu\text{-}\eta^2\text{-HN=NMe}$ complexes **2b** or **3b**, reduction of the phenyl analogue **3a** in the presence of acid leads to N=N bond cleavage. Evidently, decoordination of the N(R) end of the ligand occurs when R is electron-withdrawing (Ph) but is disfavoured when R is electron-releasing (Me). Thus, the N=N bond of a $\mu\text{-}\eta^2\text{-HN=NR}$ ligand is reductively cleaved only when circumstances permit N(R) decoordination. Otherwise, $\mu\text{-}\eta^2$ coordination could be a dead-end as far as N=N bond cleavage is concerned.

Reduction of **1b** and **3a** to complexes **4** or **5** may proceed via the bridging-imide derivative (Scheme 11; the reactions producing H_2 are not indicated). The number of electrons involved in both reduction steps depends on whether the N–N bond cleaves in $[\text{Mo}_2\text{Cp}_2(\mu\text{-SMe})_3(\mu\text{-}\eta^1\text{-NHNH}_2\text{R})]^+$ (see Scheme 7, step C) or after one-electron reduction of the latter (see Scheme 7, step D). All the complexes in Scheme 11 have been fully characterised and pathways for their conversion are now firmly established.

The $\mu\text{-}(\text{NNR}) \rightarrow [\mu\text{-}(\text{RNNH}^+) \text{ or } (\mu\text{-NN}(\text{R})\text{H}^+)] \rightarrow \mu\text{-}(\text{NH}^+)^0 \rightarrow \mu\text{-}(\text{NH}_2) \rightarrow \text{NH}_3$ protonation and reduction steps^[26–30] in Scheme 11 involve dinuclear counterparts of several intermediates involved in the Chatt cycle for mononuclear $\{\text{MP}_4\}$ complexes^[7, 12, 55] and in the Schrock cycle for $\{\text{M}(\text{Cp}^*)\text{Me}_3\}$ complexes,^[16] (M = Mo or W; P = phosphine). Therefore, most of the arguments against the participation of two (or more) metal centres in the dinitrogen reduction process can be dismissed on the basis of the chemistry established for compounds possessing a compact and robust dinuclear sulfur



Scheme 10. ● = MoCp.



Scheme 11. ● = MoCp.

core such as $\{[\text{Mo}_2\text{Cp}_2(\mu\text{-SMe})_3]^+\}$. In many respects, the chemistry of the $\{[\text{Mo}_2\text{Cp}_2(\mu\text{-SMe})_3]^+\}$ complexes is closer to that of mononuclear compounds, particularly of the ‘‘Schrock-type’’ $\{[\text{M}(\text{Cp}^*)(\text{Me}_n)]\}$ ($\text{M} = \text{Mo}, \text{W}; n = 3, 4$),^[16, 43] than to that of linear dinuclear species of the $\text{M}(\mu\text{-N}_2\text{H}_x)\text{M}$ type. Like $\{[\text{M}(\text{Cp}^*)(\text{Me}_3)]\}$,^[16] $\{[\text{Mo}_2\text{Cp}_2(\mu\text{-SMe})_3]^+\}$ offers two adjacent coordination sites and several orbitals for substrate-binding, which allow η^1/η^2 rearrangements of $\text{N}=\text{N}-\text{R}$ ligands. The flexibility of the $\{[\text{Mo}_2\text{Cp}_2(\mu\text{-SMe})_3]^+\}$ core allows different coordination geometries of the substrate. The crystal structures of the dicarbonyl,^[56] of the $\mu\text{-}\eta^1$ -diazenido,^[27] $\mu\text{-}\eta^2$ -diazene,^[27, 30] and μ -amido^[26] complexes demonstrate that only minor variations of the $\{[\text{Mo}_2\text{Cp}_2(\mu\text{-SMe})_3]^+\}$ core dimensions are sufficient to accommodate the different electronic properties and the different coordination modes of the substrates.

It is shown in Scheme 11 that several steps of the reduction of N_2 can take place at the conserved $\{[\text{Mo}_2\text{Cp}_2(\mu\text{-SMe})_3]^+\}$ site. Thus, it is tempting to propose a mechanism, similar to those presented in the Chatt and Schrock cycles, in which all of the steps of the conversion of N_2 to NH_3 occur at this site. However, coordination of N_2 at the $\{[\text{Mo}_2\text{Cp}_2(\mu\text{-SMe})_3]^+\}$ site has not been observed thus far. Nevertheless, several $[\text{Mo}_2\text{Cp}_2(\mu\text{-SMe})_3(\text{Y}=\text{Z})_2]^+$ complexes are known $[\text{Y}=\text{Z} = \text{CO}, \text{RCN}$ ($\text{Me}, \text{Et}, \text{Ph}$), RNC ($\text{R} = \text{t-Bu}, \text{PhCH}_2$)],^[18d, 56, 57] in which the π -accepting properties of the $\text{Y}=\text{Z}$ ligand, isoelectronic with N_2 , range from strong ($\text{Y}=\text{Z} = \text{CO}$)^[56] to moderate ($\text{Y}=\text{Z} = \text{MeCN}$)^[18d]. It is conceivable that an isostructural bis-dinitrogen complex may be obtained. Alternatively, a dimolybdenum μ -dinitrogen complex, in which the N_2 ligand would adopt the $(\mu\text{-}\eta^1:\eta^2)$ binding mode recently discovered by Fryzuk et al.^[58] is a reasonable possibility since in $\{[\text{Mo}_2\text{Cp}_2(\mu\text{-SMe})_3]^+\}$ complexes, the isoelectronic vinylidene fragment is coordinated in a $(\mu\text{-}\eta^1:\eta^2)$ fashion to the metal centres.^[59] Compared to the chemistry of mononuclear complexes of the Chatt type, that of the dinuclear $\{[\text{Mo}_2\text{Cp}_2(\mu\text{-SMe})_3]^+\}$, or more generally $\{[\text{M}_2(\mu\text{-SR})_n]\}$, compounds is still in its infancy, so that the synthesis of a derivative where N_2

is bound to this type of site(s) may only be a matter of time. Studies are continuing in our group to meet this objective.

Relevance to the reduction of dinitrogen at a dinuclear site in nitrogenase: In the MoFe protein N_2 most probably binds at a metal–sulfur site of the FeMo cofactor. The binding site may be di- or polynuclear. In contrast, among the many $\text{M}-\text{S}$ complexes synthesised to model the functions of nitrogenase, only very few are able to bind dinitrogen.^[61] Although most synthetic compounds^[5, 55, 60] (and the isolated FeMoco^[62]) cannot achieve this crucial step, studies using such deficient models nevertheless ‘‘can contribute meaningfully to our understanding of bioinorganic systems’’.^[63]

Only a few model studies related to biological N_2 fixation mention the involvement of a di- or polynuclear site at some stage of a reduction process mediated by synthetic complexes.^[4, 5, 15, 20, 31] It has been proposed^[5a,b] that the first steps of the biological dinitrogen reduction ($4\text{H}^+ + 4\text{e}$ reduction of N_2 to N_2H_4) could take place at an iron face of FeMoco. This would be followed by a change of coordinated hydrazine to a terminal binding mode or by migration of the hydrazine molecule from the Fe site to the Mo site where the final reduction steps could take place.^[5a,b] While the migration is a possibility, the present results suggest that, if the binding and the first N_2 reduction steps occur at a multimetallic iron site, the entire reduction might proceed at such a site.

Another possibility, which involves the opening of FeMoco on turning over, has been presented by Sellmann for the reduction of N_2 by nitrogenase.^[4b–d] The chemistry of a range of iron-thiolate compounds, including a dinuclear diazene complex $\text{Fe}(\mu\text{-H}-\text{N}=\text{N}-\text{H})\text{Fe}$, led Sellmann et al to propose a hypothetical cycle for dinitrogen reduction. As mentioned above (see Introduction), the fact that the metal centres are bridged only by the substrate results in the cleavage of the dinuclear compound at the hydrazine stage, so that only the reduction of the $(\mu\text{-N}_2)$ and that of the $(\mu\text{-H}-\text{N}=\text{N}-\text{H})$ species occur at a dinuclear centre.

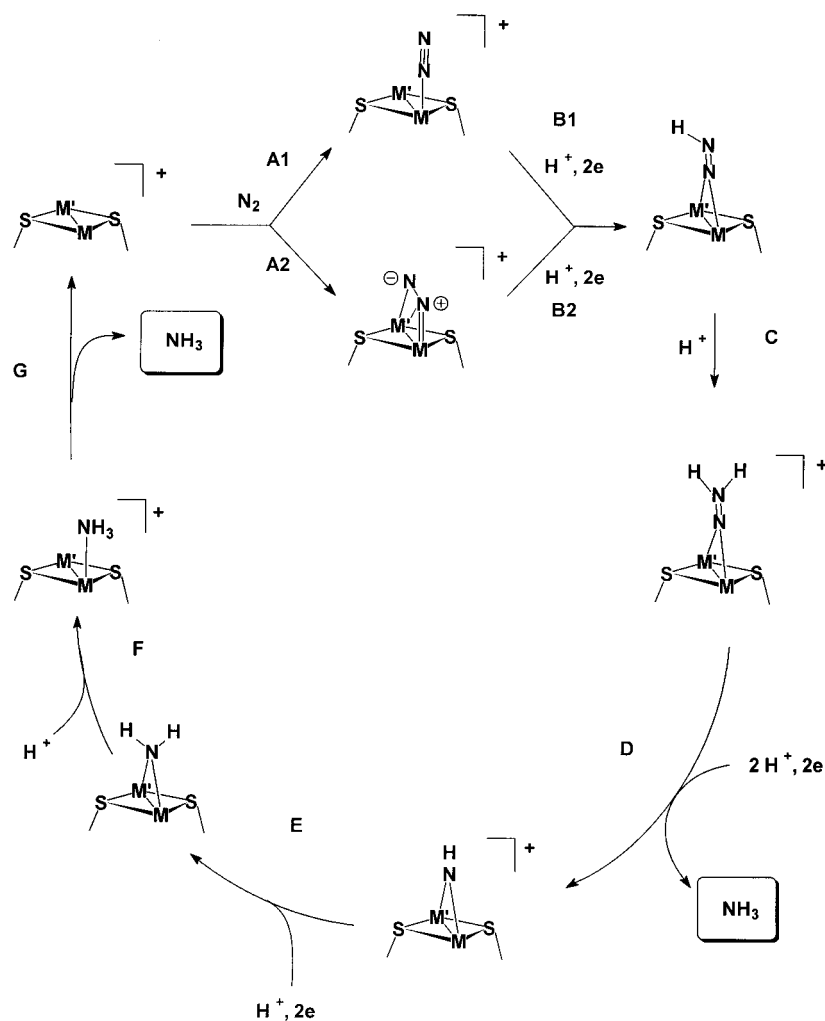
We now propose a pathway in which all of the steps of the reduction of dinitrogen occur at a *dinuclear* metal–sulfur site (Scheme 12). Durrant^[23] recently suggested that the reduction of N₂ could take place at a Mo(μ -S)₂Fe face of the cofactor.

Step A1 in Scheme 12 could result from the partial dissociation of the homocitrate ligand at the Mo centre of FeMoco allowing N₂ binding,^[6, 7, 23] or from the binding of N₂ at a single Fe atom.^[64] The first reduction step (step B1) would be analogous to the reactions observed upon reduction of [Mo₂Cp₂(μ -SMe)₃(MeCN)₂]⁺, that is transformation of one MeCN ligand from terminal to a μ - η^1 -bridging azavinylidene, with elimination of the second MeCN ligand.^[65]

An alternative possibility for steps A and B is that N₂ binds to both metal centres in the Fryzuk mode^[58] (step A2). The (2e, 1H⁺) reduction of a complex in which a vinylidene fragment is bound to the {[Mo₂Cp₂(μ -SMe)₃]⁺ core in the μ - η^1 : η^2 -mode produces a μ - η^1 -carbyne derivative.^[66] A similar structural change associated with the (2e, 1H⁺) reduction of the μ - η^1 : η^2 -N₂ complex would afford the μ - η^1 -diazenido derivative (Scheme 12, step B2).

The other steps in Scheme 12 have chemical precedents at the {[Mo₂Cp₂(μ -SMe)₃]⁺ site, although with substituted analogues for steps C and D.^[27, 30] Displacement of NH₃ from Mo by a CF₃CO₂⁻ ion (Scheme 3) could mimic the release of ammonia from the molybdenum centre in FeMoco by recoordination of the homocitrate ligand. This would restore the initial situation (Scheme 12, step G).

The sequence of transformations of the dinitrogen ligand shown in Scheme 12 are quite different from those proposed in which N₂ (or its reduced forms) is the only bridge between the metal centres. The mechanism in Scheme 12 also differs from that proposed by Durrant, which involves the rearrangement of a Mo-bound linear hydrazido(2-) ligand to a Mo/Fe μ - η^2 -bridging coordination.^[23] On the basis of the results presented here, it seems equally reasonable to suggest that a μ - η^1 -bridging hydrazido(2-) may be involved as an intermediate. The reduction could then proceed to bridging-imide and -amide species (see Scheme 7). This would circumvent the formation of the very stable^[23] molybdenum–nitride bond. This possibility strengthens the case for proposing that a dinuclear site is used in the biological process.



Scheme 12. Proposed cycle for the reduction of N₂ at a dinuclear M–S site.

Experimental Section

General: All of the experiments were carried out under an inert atmosphere, with Schlenk techniques for the syntheses. Tetrahydrofuran (THF) was purified as described previously.^[29] The acids, *p*-toluenesulfonic acid monohydrate (Aldrich) and trifluoroacetic acid (Aldrich), were used as received. The preparation and the purification of the supporting electrolyte [NBu₄][PF₆] and the electrochemical equipment were as described previously.^[29] All of the potentials (text, table, figures) are quoted against the ferrocene–ferrocenium couple; ferrocene was added as an internal standard at the end of the experiments. ¹H NMR spectra were recorded on a Bruker AC300 spectrometer. Gas chromatography was performed on a DaNI Educational chromatograph, using a SPB5 SUPELCO apolar column. UV/Vis spectra were recorded with a UV-2101PC spectrometer. Analyses for methylammonium were done using the procedure of Dubin^[67] by measuring the optical density of the sample at $\lambda = 357$ nm. [Mo₂Cp₂(μ -SMe)₃(μ - η^1 -NNHR)]⁺ (R = Me, **1b**; R = Ph, **1a**) and [Mo₂(cp)₂(μ -SMe)₃(μ - η^2 -HNNR)]⁺ (R = Me, **2b** and **3b**; R = Ph, **2a** and **3a**) were obtained following reported procedures.^[27, 30]

Controlled-potential reduction of [Mo₂Cp₂(μ -SMe)₃(μ - η^2 -HNNPh)]⁺ (3a**) in the presence of acid: aniline analysis:** In a typical experiment, **3a** (0.0073 g, 1.11 $\times 10^{-5}$ mol) was dissolved in THF/[NBu₄][PF₆]. After addition of CF₃CO₂H (5 equiv), the solution was electrolyzed (Pt cathode) at -1.8 V versus Fc^{+/0}/Fc. After passage of 4.3 F mol⁻¹ **3a**, the current fell to the background level. The catholyte was transferred in a Schlenk tube and the solution volume adjusted to 10 mL. This solution was subjected to gas chromatographic analysis for aniline. The amount of aniline present (0.068 g L⁻¹ i.e. 66% of the maximum amount on average of three injections) was quantified using a calibration curve.

Controlled-potential reduction of $[\text{Mo}_2\text{Cp}_2(\mu\text{-SMe})_3(\mu\text{-}\eta^1\text{-NNHMe})]^+$ (1b**) in the presence of acid: methylammonium analysis:** In a typical experiment, $[\text{Mo}_2\text{Cp}_2(\mu\text{-SMe})_3(\mu\text{-}\eta^1\text{-NNHMe})]^+$ **1b** (0.0034 g, 5.7×10^{-6} mol) and a diluted THF solution ($4.4 \mu\text{L}$, 1.90×10^{-5} mol, 3.3 equiv) of $\text{CF}_3\text{CO}_2\text{H}$ (4.3×10^{-6} mol μL^{-1}) in $\text{THF}/[\text{NBu}_4][\text{BF}_4]$ (2.5 mL) were electrolysed at -2 V versus Fc^+/Fc (graphite cathode). The electrolysis was stopped after the passage of 4.1 F mol^{-1} **1b**. 0.15 mL of the catholyte was used to quantify the amount of methylamine formed during the electrolysis (2.5×10^{-6} mol MeNH_3^+ , about 44% of the maximum amount possible), according to the Dubin procedure.^[67]

Acknowledgements

The authors thank CNRS (France), EPSRC (UK), the Université de Bretagne Occidentale, and Glasgow University for financial support. The Conseil Régional de Bretagne is acknowledged for financial support to this work (PRIR, Operation n° 98CCO9) and for providing a studentship to N.L.G. The authors are grateful to L. Stéphan for gas chromatographic analysis of aniline.

- [1] a) J. Kim, D. C. Rees, *Science* **1992**, 257, 1677; b) J. Kim, D. C. Rees, *Nature* **1992**, 360, 553; c) M. K. Chan, J. Kim, D. C. Rees, *Science* **1993**, 260, 792; d) D. C. Rees, J. Kim, M. M. Georgiadis, H. Komiya, A. J. Chirino, D. Woo, J. Schlessman, M. K. Chan, L. Joshua-Tor, G. Santillan, P. Chakrabarty, B. T. Hsu in *Molybdenum Enzymes, Cofactors, and Model Systems* (Eds.: E. I. Stiefel, D. Coucouvanis, W. E. Newton), ACS Symposium Series 535, **1993**, Chapter 11, 170.
- [2] J. T. Bolin, N. Campobasso, S. W. Muchmore, T. V. Morgan, L. E. Mortenson in *Molybdenum Enzymes, Cofactors, and Model Systems*, (Eds.: E. I. Stiefel, D. Coucouvanis, W. E. Newton), ACS Symposium Series 535, **1993**, Chapter 12, 187.
- [3] W.H Orme-Johnson, *Science* **1992**, 257, 1639.
- [4] a) D. Sellmann, *Angew. Chem.* **1993**, 105, 67; *Angew. Chem. Int. Ed. Engl.* **1993**, 32, 64; b) D. Sellmann, J. Sutter, *J. Biol. Inorg. Chem.* **1996**, 1, 587; c) D. Sellmann, J. Sutter, *Acc. Chem. Res.* **1997**, 30, 460; d) D. Sellmann, J. Utz, N. Blum, F. W. Heinemann, *Coord. Chem. Rev.* **1999**, 190–192, 607.
- [5] a) D. Coucouvanis, *J. Biol. Inorg. Chem.* **1996**, 1, 594; b) K. Demadis, S. Malinak, D. Coucouvanis, *Inorg. Chem.* **1996**, 35, 4038; c) D. Coucouvanis in *Molybdenum Enzymes, Cofactors, and Model Systems* (Eds.: E. I. Stiefel, D. Coucouvanis, W. E. Newton), ACS Symposium Series 535, **1993**, Chapter 20, 305; d) D. Coucouvanis, K. D. Demadis, S. M. Malinak, P. E. Mosier, M. A. Tyson, L. J. Laughlin, *J. Mol. Catal.* **1996**, 107, 123.
- [6] D. L. Hughes, S. K. Ibrahim, G. Querné, A. Laouénan, J. Talarmin, A. Queiros, A. Fonseca, C. J. Pickett, *Polyhedron* **1994**, 13, 3341.
- [7] C. J. Pickett, *J. Biol. Inorg. Chem.* **1996**, 1, 601.
- [8] H. Deng, R. Hoffmann, *Angew. Chem.* **1993**, 105, 1125; *Angew. Chem. Int. Ed. Engl.* **1993**, 32, 1062.
- [9] a) I. G. Dance, *Aust. J. Chem.* **1994**, 47, 979; b) I. G. Dance, *J. Biol. Inorg. Chem.* **1996**, 1, 581; c) I. G. Dance, *Chem. Commun.* **1997**, 165.
- [10] K. K. Stavrev, M. C. Zerner, *Chem. Eur. J.* **1996**, 2, 83.
- [11] S.-J. Zhong, C.-W. Liu, *Polyhedron* **1997**, 16, 653.
- [12] J. Chatt, J. R. Dilworth, R. L. Richards, *Chem. Rev.* **1978**, 78, 589 and references therein.
- [13] R. A. Henderson, G. J. Leigh, C. J. Pickett, *Adv. Inorg. Chem. Radiochem.* **1983**, 27, 197 and references therein.
- [14] M. Hidai, Y. Mizobe, *Chem. Rev.* **1995**, 95, 1115 and references therein.
- [15] T. A. Bazhenova, A. E. Shilov, *Coord. Chem. Rev.* **1995**, 144, 69 and references therein.
- [16] a) R. R. Schrock, *Pure Appl. Chem.* **1997**, 69, 2197; b) R. R. Schrock, T. E. Glassman, M. G. Vale, M. Kol, *J. Am. Chem. Soc.* **1993**, 115, 1760; c) T. E. Glassman, M. G. Vale, R. R. Schrock, *J. Am. Chem. Soc.* **1992**, 114, 8098; d) T. E. Glassman, A. H. Liu, R. R. Schrock, *Inorg. Chem.* **1991**, 30, 4723; e) R. R. Schrock, T. E. Glassman, M. G. Vale, *J. Am. Chem. Soc.* **1991**, 113, 725; f) T. E. Glassman, M. G. Vale, R. R. Schrock, *Organometallics* **1991**, 10, 4046; g) M. B. O'Regan, A. H. Liu, W. C. Finch, R. R. Schrock, W. M. Davis, *J. Am. Chem. Soc.* **1990**, 112, 4331; h) R. R. Schrock, R. M. Kolodziej, A. H. Liu, W. M. Davis, M. G. Vale, *J. Am. Chem. Soc.* **1990**, 112, 4338.
- [17] a) C. E. Laplaza, C. C. Cummins, *Science* **1995**, 268, 861; b) C. E. Laplaza, M. J. A. Johnson, J. C. Peters, A. L. Odom, E. Kim, C. C. Cummins, G. N. George, I. J. Pickering, *J. Am. Chem. Soc.* **1996**, 118, 8623; c) for references concerning bridging N_2 complexes see reference 9 in ref. [16b]).
- [18] a) F. Y. Pétilion, P. Schollhammer, J. Talarmin, K. W. Muir, *Coord. Chem. Rev.* **1998**, 178–180, 203; b) F. Y. Pétilion, P. Schollhammer, J. Talarmin, *J. Organomet. Chem.* **1991**, 411, 159; c) F. Gloaguen, C. Le Floch, F. Y. Pétilion, J. Talarmin, M. El Khalifa, J. Y. Saillard, *Organometallics* **1991**, 10, 2004; d) F. Barrière, Y. Le Mest, F. Y. Pétilion, S. Poder-Guillou, P. Schollhammer, J. Talarmin, *J. Chem. Soc. Dalton Trans.* **1996**, 3967; e) F. Y. Pétilion, S. Poder-Guillou, P. Schollhammer, J. Talarmin, *New J. Chem.* **1997**, 21, 477; f) M. L. Abasq, D. L. Hughes, F. Y. Pétilion, R. Pichon, C. J. Pickett, J. Talarmin, *J. Chem. Soc. Dalton Trans.* **1997**, 2279; g) P. Madec, K. W. Muir, F. Y. Pétilion, R. Rumin, Y. Scaon, P. Schollhammer, J. Talarmin, *J. Chem. Soc. Dalton Trans.* **1999**, 2371.
- [19] a) G. J. Kubas, P. J. Vergamini, *Inorg. Chem.* **1981**, 20, 2667; b) P. J. Vergamini, G. J. Kubas, *Inorg. Chem.* **1976**, 21, 261.
- [20] a) S. Kuwata, Y. Mizobe, M. Hidai, *Inorg. Chem.* **1994**, 33, 3619; b) H. Matsuzaka, H. Koizumi, Y. Takagi, M. Nishio, M. Hidai, *J. Am. Chem. Soc.* **1993**, 115, 10396; c) S. Dev, Y. Mizobe, M. Hidai, *Inorg. Chem.* **1990**, 29, 4797.
- [21] R. W. F. Hardy, R. C. Burns, G. W. Parshall, *ACS Symposium Series* **1971**, 100, 219.
- [22] G. J. Leigh, *Eur. J. Biochem.* **1995**, 229, 14; b) R. R. Eady, G. J. Leigh, *J. Chem. Soc. Dalton Trans.* **1994**, 2739.
- [23] M. C. Durrant, *Inorg. Chem. Commun.* **2001**, 4, 60.
- [24] It has been shown that the sulfur bridges in related dimolybdenum complexes can also play an active part in the reduction of substrates.^[25]
- [25] a) M. Rakowski DuBois, *Chem. Rev.* **1989**, 89, 1; b) P. Bernatis, J. C. V. Laurie, M. Rakowski DuBois, *Organometallics* **1990**, 9, 1607; c) C. J. Casewit, D. E. Coons, L. L. Wright, W. K. Miller, M. Rakowski DuBois, *Organometallics* **1986**, 5, 951; d) M. Rakowski DuBois, M. C. Vanderveer, D. L. DuBois, R. C. Haltiwanger, W. K. Miller, *J. Am. Chem. Soc.* **1980**, 102, 7456.
- [26] P. Schollhammer, F. Y. Pétilion, S. Poder-Guillou, J. Y. Saillard, J. Talarmin, K. W. Muir, *Chem. Commun.* **1996**, 2633.
- [27] P. Schollhammer, E. Guénin, F. Y. Pétilion, J. Talarmin, K. W. Muir, D. Yufit, *Organometallics* **1998**, 17, 1922.
- [28] F. Y. Pétilion, P. Schollhammer, J. Talarmin, *J. Chem. Soc. Dalton Trans.* **1997**, 4019.
- [29] J. Y. Cabon, K. W. Muir, F. Y. Pétilion, F. Quantel, P. Schollhammer, J. Talarmin, *Chem. Eur. J.* **2000**, 6, 3033.
- [30] P. Schollhammer, B. Didier, N. Le Grand, F. Y. Pétilion, J. Talarmin, K. W. Muir, S. J. Teat, *Eur. J. Inorg. Chem.* **2002**, 3, 658.
- [31] F. Y. Pétilion, P. Schollhammer, J. Talarmin, K. W. Muir, *Inorg. Chem.* **1999**, 38, 1954.
- [32] The parameters i_p and E_p are the peak current and the peak potential of a redox process, respectively; $E_{1/2} = (E_p^a - E_p^c)/2$; E_p^a , i_p^a and E_p^c , i_p^c are respectively the potential and the current of the anodic and of the cathodic peak of a reversible process; an EC process comprises an electron transfer step (E) followed by a chemical reaction (C). CV and CPE stand for cyclic voltammetry and controlled-potential electrolysis, respectively.
- [33] The shoulder on the oxidation peak of **3a** (see Figure 1, 3a, 5a) is due to the second phenyldiazene isomer, **2a**, the oxidatively-induced isomerisation of **3a** is suppressed at low temperature.^[34]
- [34] F. Y. Pétilion, P. Schollhammer, J. Talarmin, K. W. Muir, unpublished results.
- [35] a) A. J. Bard, L. R. Faulkner, *Electrochemical Methods. Fundamentals and Applications*, Wiley, New York, **1980**, chapter 11, pp. 429–485; b) E. R. Brown, R. F. Large in *Techniques of Chemistry, Volume I - Physical Methods of Chemistry, Part IIA* (Ed.: A. Weissberger), Wiley, **1971**, chapter 6, pp. 423–530.
- [36] a) R. S. Nicholson, I. Shain, *Anal. Chem.* **1964**, 36, 706; b) R. S. Nicholson, *Anal. Chem.* **1966**, 38, 1406.
- [37] The yield was calculated from the ratio of the one-electron oxidation peak current of the product to the one-electron oxidation peak current

- of **3a** before electrolysis, assuming identical diffusion coefficients for both complexes.
- [38] The design of the electrochemical cell used throughout did not allow H₂ detection because a dinitrogen or argon stream was continuously circulating over the solution during the experiments.
- [39] R. S. Nicholson, I. Shain, *Anal. Chem.* **1965**, *37*, 179; R. S. Nicholson, I. Shain, *Anal. Chem.* **1965**, *37*, 190.
- [40] T. I. Al-Salih, C. J. Pickett, R. L. Richards, J. Talarmin, A. J. L. Pombeiro, *Port. Electrochim. Acta* **1985**, *3*, 35.
- [41] M. Le Hénañf, C. Le Roy-Le Floch, K. W. Muir, F. Y. Pétillon, P. Schollhammer, J. Talarmin, unpublished results.
- [42] The peak separation of the quasireversible reduction of **3a** ($\Delta E_p = 80$ mV, -40°C ; compare with $\Delta E_p = 80$ mV for ferrocene) suggests that if a structural change occurs concomitantly with the electron transfer, the former is fast and reversible. The structural change following the electron transfer generates **I**.
- [43] R. R. Schrock, A. H. Liu, M. B. O'Regan, W. C. Finch, J. F. Payack, *Inorg. Chem.* **1988**, *27*, 3574.
- [44] P. D. Frish, M. M. Hunt, W. G. Kita, J. A. McCleverty, A. E. Rae, D. Seddon, D. Swann, J. Williams, *J. Chem. Soc. Dalton Trans.* **1979**, 1819.
- [45] I. A. Latham, G. J. Leigh, G. Hüttner, I. Jibril, *J. Chem. Soc. Dalton Trans.* **1986**, 385.
- [46] F. P. O'Flaherty, R. A. Henderson, D. L. Hughes, *J. Chem. Soc. Dalton Trans.* **1990**, 1087.
- [47] K. W. Kramarz, J. R. Norton, *Prog. Inorg. Chem.* **1994**, *42*, 1.
- [48] W. J. Evans, G. Kociok-Köhn, V. S. Leong, J. W. Ziller, *Inorg. Chem.* **1992**, *31*, 3592.
- [49] J. R. Dilworth, R. A. Henderson, P. Dahlstrom, T. Nicholson, J. A. Zubietta, *J. Chem. Soc. Dalton Trans.* **1987**, 529.
- [50] J. A. McCleverty, A. E. Rae, I. Wolochowicz, N. A. Bailey, J. M. A. Smith, *J. Chem. Soc. Dalton Trans.* **1983**, 71.
- [51] D. Sellmann, W. Kern, G. Pöhlmann, F. Knoch, M. Moll, *Inorg. Chim. Acta* **1991**, *185*, 155.
- [52] C. Bustos, C. Manzur, D. Carrillo, F. Robert, P. Gouzerh, *Inorg. Chem.* **1994**, *33*, 1427.
- [53] P. Schollhammer, M. Le Hénañf, C. Le Roy-Le Floch, F. Y. Pétillon, J. Talarmin, K. W. Muir, *J. Chem. Soc. Dalton Trans.* **2001**, 1573.
- [54] It must be noted that for **1b**, the ratio of the reduction peak current measured in the presence of an excess acid (about 4 equiv) to the reduction peak current measured in the absence of acid for **1b**, $i_p^{\text{red}}(\text{H}^+)/i_p^{\text{red}} \gg 2$. This suggests that the slow step detected in the reduction of **3a** (see Figure 2) in the presence of acid does not take place for **1b**. This would be entirely consistent with the slow step in the reduction of **3a** being a $\mu\text{-}\eta^2 \rightarrow \mu\text{-}\eta^1$ rearrangement of the protonated NN ligand (see Scheme 7).
- [55] R. L. Richards, *Coord. Chem. Rev.* **1996**, *154*, 83.
- [56] M. B. Gomes de Lima, J. E. Guerschais, R. Mercier, F. Y. Pétillon, *Organometallics* **1986**, *5*, 1952.
- [57] P. Schollhammer, K. W. Muir, F. Y. Pétillon, J. Talarmin, unpublished results.
- [58] a) M. D. Fryzuk, S. A. Johnson, S. J. Rettig, *J. Am. Chem. Soc.* **1998**, *120*, 11024; M. D. Fryzuk, S. A. Johnson, *Coord. Chem. Rev.* **2000**, *200–202*, 379.
- [59] P. Schollhammer, N. Cabon, J.-F. Capon, F. Y. Pétillon, J. Talarmin, K. W. Muir, *Organometallics* **2001**, *20*, 1230.
- [60] P. B. Hitchcock, D. L. Hughes, M. J. McGuire, K. Marjani, R. L. Richards, *J. Chem. Soc. Dalton Trans.* **1997**, 4747.
- [61] D. Sellmann, B. Hautsch, A. Rösler, F. W. Heinemann, *Angew. Chem.* **2001**, *113*, 1553; *Angew. Chem. Int. Ed.* **2001**, *40*, 1505.
- [62] B. K. Burgess, *Chem. Rev.* **1990**, *90*, 1377.
- [63] R. A. Henderson, *J. Chem. Soc. Dalton Trans.* **1995**, 503.
- [64] T. H. Rod, J. K. Nørskov, *J. Am. Chem. Soc.* **2000**, *122*, 12751.
- [65] P. Schollhammer, N. Cabon, F. Y. Pétillon, J. Talarmin, K. W. Muir, *Chem. Commun.* **2000**, 2137.
- [66] N. Cabon, K. W. Muir, F. Y. Pétillon, P. Schollhammer, J. Talarmin, unpublished results.
- [67] D. T. Dubin, *J. Biol. Chem.* **1960**, *235*, 783.

Received: January 30, 2002
Revised: March 14, 2002 [F3837]